

1 **Differential cortical and subcortical visual processing with eyes shut**

2
3
4

5 **Author names and affiliations:** Nicholas G. Cicero^{1,3,4}, Michaela Klimova², Laura D.
6 Lewis^{3,4,5,6}, & Sam Ling^{1,2,6}

7 ¹Graduate Program in Neuroscience, Boston University; ²Department of Psychological
8 and Brain Sciences, Boston University; ³Department of Biomedical Engineering, Boston
9 University; ⁴Institute for Medical Engineering and Sciences, Massachusetts Institute of
10 Technology; ⁵Department of Electrical Engineering and Computer Science,
11 Massachusetts Institute of Technology; ⁶Athinoula A. Martinos Center for Biomedical
12 Imaging, Department of Radiology, Massachusetts General Hospital

13

14 **Author list footnotes:** ⁶Lead contact

15

16 **Corresponding author email address:** samling@bu.edu and ldlewis@mit.edu

17

18 **Conflict of interest statement:** The authors declare no competing financial interests.

19

20 **Acknowledgements:** This work was supported by National Institutes of Health R01
21 EY028163 to S.L., the Sloan Fellowship, McKnight Scholar Award, Pew Biomedical
22 Scholar Award and NIH U19- NS128613 to L.D.L. This research was carried out at the
23 Boston University Cognitive Neuroimaging Center. This work involved the use of
24 instrumentation supported by the NSF Major Research Instrumentation grant BCS-
25 1625552. We acknowledge the University of Minnesota Center for Magnetic Resonance
26 Research for use of the multiband-EPI pulse sequences. Data was analyzed on a high-
27 performance computing cluster supported by the ONR grant N00014-17-1-2304. We
28 thank Shruthi Chakrapani and Stephanie McMains for assistance with data collection, and
29 members of the S.L. laboratory and L.D.L. laboratory for helpful feedback on the
30 manuscript.

31 **Significance statement**

32 When we close our eyes, not all information is blocked out. Coarse luminance information
33 is still accessible for processing by the visual system, even when our eyes are closed.
34 Using functional magnetic resonance imaging (fMRI), we examined whether eyelid
35 closure plays a unique role in visual processing. We discovered that while the thalamus
36 and primary visual cortex (V1) show equivalent luminance-dependent responses both
37 when the eyes are open and closed, extrastriate cortex exhibited a qualitatively distinct
38 pattern of responses. Specifically, eye closure attenuated luminance responses in
39 extrastriate cortices, but responses were preserved in LGN and V1. This pattern suggests
40 that during brain states where the eyes are closed, visual information is still accessible to
41 the very earliest stages of visual processing, but that downstream visual processing areas
42 appear to become blind to this information.

43 **Abstract**

44 Closing our eyes largely shuts down our ability to see. That said, our eyelids still pass
45 some light, allowing our visual system to coarsely process information about visual
46 scenes, such as changes in luminance. However, the specific impact of eye closure on
47 processing within the early visual system remains largely unknown. To understand how
48 visual processing is modulated when eyes are shut, we used functional magnetic
49 resonance imaging (fMRI) to measure responses to a flickering visual stimulus at high
50 (100%) and low (10%) temporal contrasts, while participants viewed the stimuli with their
51 eyes open or closed. Interestingly, we discovered that eye closure produced a
52 qualitatively distinct pattern of effects across the visual thalamus and visual cortex. We
53 found that with eyes open, low temporal contrast stimuli produced smaller responses,
54 across the lateral geniculate nucleus (LGN), primary (V1) and extrastriate visual cortex
55 (V2). However, with eyes closed, we discovered that the LGN and V1 maintained similar
56 BOLD responses as the eyes open condition, despite the suppressed visual input through
57 the eyelid. In contrast, V2 and V3 had strongly attenuated BOLD response when eyes
58 were closed, regardless of temporal contrast. Our findings reveal a qualitative distinct
59 pattern of visual processing when the eyes are closed – one that is not simply an overall
60 attenuation, but rather reflects distinct responses across visual thalamocortical networks,
61 wherein the earliest stages of processing preserves information about stimuli but is then
62 gated off downstream in visual cortex.

63

64 keywords: luminance, fMRI, eyelid, visual cortex, LGN

65 Introduction

66

67 Light exposure during sleep has substantial effects on the brain: it can alter circadian
68 rhythms, sleep quality, and mood (Blume et al., 2019; Ohayon & Milesi, 2016). During
69 sleep, our eyes are closed and the eyelids function as potent filters of visual information.
70 However, our eyelids are only partial filters and do not completely attenuate all visual
71 information (Ando & Kripke, 1996; Bierman et al., 2011). The eyelid has been
72 characterized as a red-pass filter, with an estimated 6% red light spectral transmittance
73 (Ando & Kripke, 1996). Indeed, subjective experience with high luminance stimuli, such
74 as during a sunny day, corroborates the idea that changes in luminance are still
75 detectable when our eyes are closed. With partial, rather than complete, filtering
76 properties, it follows that the visual system processes external visual information with our
77 eyes closed, as well.

78 How does the visual system process information when our eyes are closed? It is
79 possible that the filtering properties of the eyelid simply quantitatively suppress responses
80 across visual regions, due to the attenuation of input. Alternatively, eye closure could
81 induce qualitatively distinct changes in visual response, selectively modulating responses
82 in specific brain networks. While little is known about stimulus-evoked visual responses
83 with eyes closed, resting-state fMRI studies have investigated spontaneous dynamics
84 during eye closure in the absence of any visual stimulus presentation (Marx et al., 2003;
85 Wei et al., 2018; Weng et al., 2020). These studies found differences in resting-state
86 functional connectivity in attentional networks depending on whether eyes were open or
87 closed, along with differences in activation in prefrontal cortex, parietal and frontal eye
88 fields, and LGN. While eye closure appears to play a unique role in modulating brain
89 responses, the impact that eye closure has on stimulus-evoked visual responses remains
90 poorly understood.

91 In this study, we sought to shed light on the role that eye closure plays in
92 modulating responses within the visual processing hierarchy. To do so, we measured
93 fMRI BOLD responses within visual cortex and subcortex while participants viewed high
94 and low intensity visual stimuli, with their eyes open or shut. We manipulated the intensity
95 of visual input via temporal contrast modulation, in which the luminance of a uniform visual

96 stimuli flickered rapidly between extreme whites and blacks (high temporal contrast), or
97 between middling intensities (low temporal contrast). Indeed, previous work has shown
98 visuocortical responses to be sensitive to changes in luminance (Vinke & Ling, 2020). By
99 measuring BOLD responses to high and low luminance contrast stimuli, we examined
100 whether there is a qualitatively unique pattern of luminance responses across the
101 visuocortical hierarchy when one's eyes are closed, compared to when they are open.

102

103 **Methods**

104

105 *Participants*

106 Data was acquired from a total of 8 healthy participants (5 females, 3 males). Participants
107 were aged 18-35 years, reported normal or corrected-to-normal visual acuity, and were
108 recruited from Boston University and the surrounding community. All participants provided
109 written informed consent before study enrollment and completed a metal screening form
110 indicating that they had no MRI contraindications. Participants were reimbursed for their
111 study participation. All aspects of the study were approved by Boston University's
112 Institutional Review Board.

113

114 *Apparatus & stimuli*

115 Stimuli were generated using custom software written in MATLAB (version 2019b) in
116 conjunction with Psychtoolbox (Brainard, 1997). Participants viewed stimuli that was
117 back-projected onto a screen set within the MRI scanner, using a ProPIXX DLP LED
118 (VPixx Technologies) projector system (minimum luminance: 1.2 cd/m²; maximum
119 luminance: 2507.9 cd/m²). Photometer measurements (model LS-100; Konica Minolta)
120 carried out before the study were used to verify the linearity of the display (1 digital-to-
121 analog conversion (DAC) step = 9.835 cd/m²). These measurements were used to
122 calculate the stimulus luminance and were acquired from the inner-facing side of the
123 back-projection screen while positioned within the MRI scanner bore. This was done to
124 best account for the attenuation in luminance due to back-projection screen
125 characteristics.

126 During each functional run, participants fixated on a median luminance crosshair
127 at the center of the display while shown a full screen flickering display (17 degrees of
128 visual angle) with no spatial contrast (Figure 1). The full field flicker was presented in a
129 block design with three trial types (baseline, high, and low temporal luminance contrast),
130 with each event lasting 16 seconds. In the *baseline* events, the full field display was a
131 constant median luminance with no luminance modulation. During *high* events, the full
132 field display flickered with an amplitude envelope of 100% around the middle luminance
133 value. For *low* events the full field display flickered with an amplitude envelope of 10%
134 around the median luminance value. All high and low events flickered at a frequency of 7
135 Hz.

136

137 *Experimental design*

138 Subjects participated in two scan sessions, each lasting approximately two hours. The
139 first session was dedicated to collecting anatomical images and data for population
140 receptive field (pRF) mapping using standard techniques and stimuli (Dumoulin &
141 Wandell, 2008; Kay et al., 2013). The second session was dedicated to collecting proton-
142 density (PD) weighted anatomical imaging and fMRI blood oxygenation level-dependent
143 (BOLD) data across the eyes open and closed conditions, during the luminance task.

144 During the second experimental session, we collected three PD-weighted
145 anatomical scans. PD-weighted anatomical imaging has previously been used to better
146 localize the LGN (Fujita et al., 2001; Ling et al., 2015). Following the PD-weighted scans,
147 participants completed three consecutive runs of a functional localizer. The visual
148 stimulus for the functional localizer contained a full field flickering grating stimulus
149 (diameter = 6.0°) with a centered circle (diameter = 0.8°). Within the centered circle,
150 letters rapidly appeared one at a time with a new letter appearing every 200 ms.
151 Participants were instructed to press a button whenever the letters 'J' and 'K' appeared
152 within the centered circle. During the localizer blocks, the full field display alternated
153 between a flickering grating stimulus and a full field non-flickering display at median
154 luminance value. Participants completed 12 total blocks (6 flickering field, 6 non-flickering
155 field) with an extra non-flickering block at the beginning of the run. At the end of each
156 localizer run, participants were asked to report their wakefulness level.

157 Participants then completed the luminance flicker task. The task began and ended
158 with a baseline event. High and low temporal contrast conditions were pseudo-randomly
159 ordered, with all high and low events interleaved with a baseline event. Each run
160 contained 12 events (6 high, 6 low) interspersed with 12 baseline events, lasting a total
161 of 384 seconds. On each run participants were instructed to press a button after each full
162 breath cycle (1 inhale, 1 exhale). This button task was chosen to ensure that participants
163 did not fall asleep and engaged with the task, while not requiring eyes to be open. For
164 each run, participants were instructed to either keep their eyes open and fixate on the
165 crosshair or to keep their eyes closed throughout the run. Each scan session began with
166 an eyes-closed run, and consecutive runs alternated between open and closed
167 conditions. We always began with the eyes closed condition to ensure we acquired a
168 sufficient number of runs in this condition, where BOLD modulations may be lower
169 compared to eyes-open runs. To ensure participants kept their eyes closed or open, real
170 time eye monitoring was carried out using an EyeLink1000, for the duration of each run.
171 On average, we collected 5 runs with eyes closed and 4 runs with eyes open, for each
172 subject.

173

174 *MRI data acquisition*

175 All neuroimaging data were acquired using a research-dedicated Siemens Prisma 3T
176 scanner using a Siemens 64-channel head coil. A whole brain anatomical scan was
177 acquired using a T1-weighted multi-echo MPRAGE (1 mm isotropic voxels; field of view
178 (FOV) = 192 x 192 x 134 mm, flip angle (FA) = 7.00°, repetition time (TR) = 2200 ms,
179 echo time (TE) = 1.57 ms). Proton density (PD)-weighted anatomical scans were acquired
180 to localize LGN (0.9mm x 0.9mm x 1.7mm; TR = 2950.0 ms; TE = 15.6 ms; FA = 180°).
181 Functional scans were acquired using T2*-weighted in-plane simultaneous imaging (2
182 mm isotropic voxels; FOV = 104 x 104 x 70 mm, FA = 64.00°, TR = 1000 ms, TE = 30
183 ms, SMS factor = 5, GRAPPA acceleration = 2).

184

185 *Anatomical data analysis*

186 T1-weighted anatomical data were analyzed using the standard “recon-all” pipeline
187 provided by the FreeSurfer neuroimaging analysis package (Fischl, 2012), generating

188 cortical surface models, whole brain segmentations, and cortical parcellations. All PD-
189 weighted scans were aligned to each subject's anatomical space and averaged together
190 (using AFNI's 3dcalc).

191

192 *Functional data analysis*

193 Functional BOLD time-series data were first corrected for echo-planar imaging (EPI)
194 distortions using a reverse phase-encode method implemented in FSL (Andersson et al.,
195 2003) and were then preprocessed with FS-FAST using standard motion-correction
196 procedures, slice timing correction, and boundary-based registration between functional
197 and anatomical spaces (Greve & Fischl, 2009). To optimize spatial precision of
198 experimental data, no volumetric spatial smoothing was performed (full-width half-
199 maximum 0 mm). To achieve precise alignment of experimental data within the session,
200 cross-run within-modality robust rigid registration was performed, using the middle time
201 point of each run (Reuter et al., 2010). BOLD time-series data were demeaned and
202 converted to units of percent signal change. Data collected during the separate pRF
203 mapping scans were analyzed using the analyzePRF toolbox (Kay et al., 2013). Results
204 from the pRF model were used to manually draw labels for our regions of interest within
205 visual cortex.

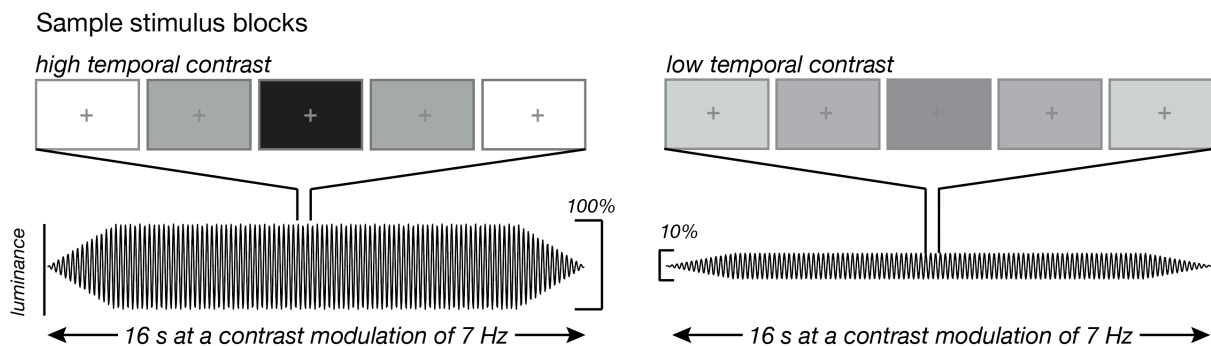
206

207 *Statistical analysis*

208 The results from the pRF modeling were used to identify region-of-interest (ROI) labels
209 for each cortical region before analysis. ROI labels included voxels located inside the
210 cortical ribbon for V1/V2/V3, which were identified using a visual area network label
211 generated using an intrinsic functional connectivity atlas (Yeo et al, 2012). Results from
212 the pRF modeling were additionally used to select voxels with visual field eccentricity
213 preferences less than 17 degrees visual angle away from fixation as this was the
214 measured extent of the screen within the MRI scanner. Cortical voxels with a poor pRF
215 model fit ($r^2 < 0.10$) were removed from further analyses. Initial LGN labels were acquired
216 from thalamic segmentation and parcellation in Free-Surfer for each participant. These
217 initial labels were overlaid with the GLM results from the functional localizer and the PD-

218 weighted scans, and only intersecting voxels from the top 40% of t-values from the
219 functional localizer were chosen for the final LGN labels and further analyses.

220 An event-triggered average was computed for each flickering condition (low and
221 high) per eyelid condition and ROI. The BOLD time-series for each ROI per run was
222 separated by the low and high trials, and all trials of a given type were averaged together.
223 Average BOLD magnitude in response to the stimulus presentation was computed by
224 averaging 4-16 s post-stimulus onset for each trial. Two-way between-subjects ANOVA
225 were performed to test for any main effects of temporal contrast and eye closure and any
226 interaction of the two on average BOLD magnitude during stimulus presentation.
227 Additional event-triggered average analysis was done with eccentricity, in which the time-
228 series for V1/V2/V3 voxels were first separated into eccentricity bins defined by degree
229 visual angle relative to fixation. Foveal-tuned voxels were between $0.01^\circ - 1.5^\circ$,
230 parafoveal-tuned voxels were between $1.5^\circ - 4.0^\circ$, and peripheral-tuned voxels were
231 between $4.0^\circ - 17.0^\circ$. An additional ANOVA was performed to test for any main effect of
232 eccentricity on BOLD response during stimulus presentation. Multiple comparison
233 correction was done using Bonferroni correction of α/n at a familywise α of 0.05 where n
234 is the number of tests performed.



235 **Figure 1. Experimental design with sample stimulus frames displaying the high temporal**
236 **contrast and low temporal contrast displays.** High temporal contrast flickered at 7 Hz with a
237 luminance amplitude envelope of 100%, encompassing the maximum (255 a.u.) and minimum (0 a.u.)
238 possible luminance values. The low temporal contrast events also flickered at 7 Hz with a luminance
239 amplitude envelope of 10%, encompassing a range of luminance values between 140 a.u. and 115
240 a.u.

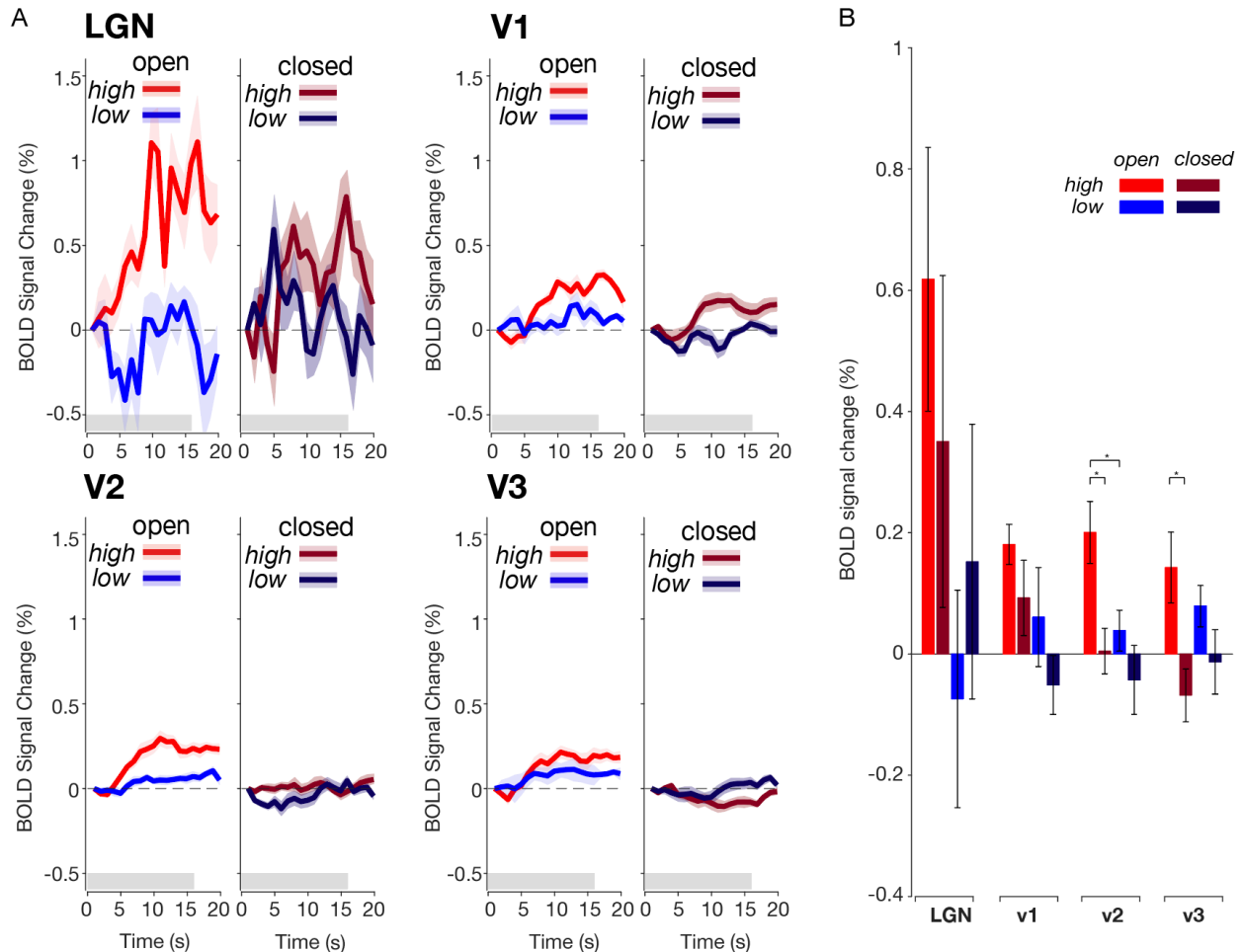
241

242 Results

243 We first examined how temporal contrast modulated thalamic and visuocortical
244 responses, and if eye closure impacted these responses. With eyes open, LGN, V1, and

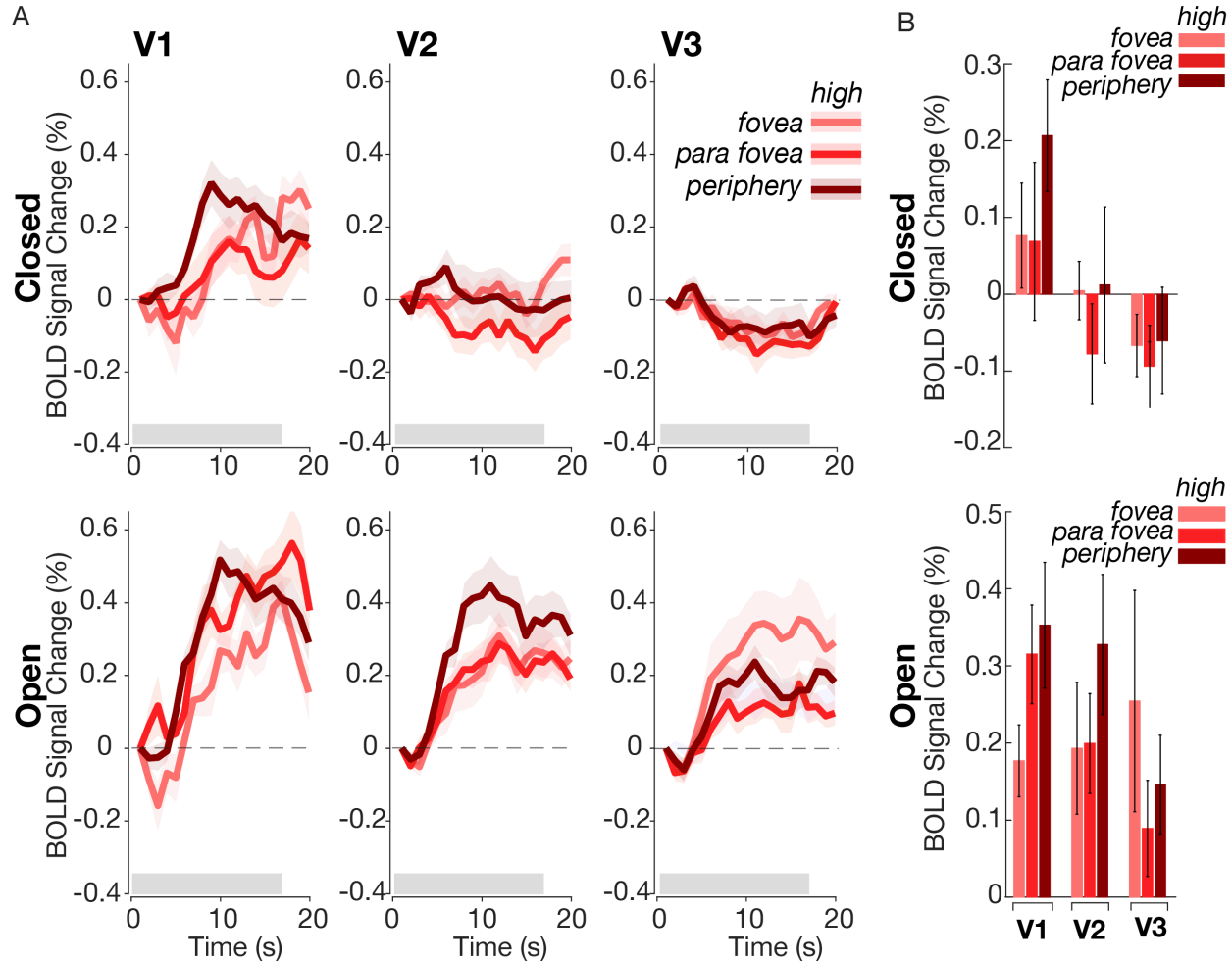
245 V2 showed larger responses to high temporal contrast stimuli, compared to low temporal
246 contrast stimuli (Figure 2A). Indeed, during eyes open with high temporal contrast stimuli,
247 all ROIs had significantly elevated BOLD responses [LGN: $t(7) = 2.84$, $P = 0.0125$; V1:
248 $t(7) = 5.45$, $P < 0.0001$; V2: $t(7) = 3.92$, $P = 0.0028$; V3: $t(7) = 2.44$, $P = 0.022$), though
249 the significant response in V3 did not survive multiple comparisons correction. When the
250 participants closed their eyes, however, LGN and V1 maintained their stronger responses
251 to higher contrast stimuli [LGN: $F(1,31) = 3.86$, $P = 0.059$; V1: $F(1,31) = 5.70$, $P = 0.023$],
252 which did not differ from their eyes closed conditions [LGN: $F(1,31) = 0.847$, $P = 0.364$;
253 V1: $F(1,31) = 3.06$, $P = 0.091$]. In other words, while responses in LGN and V1 were
254 significantly modulated by temporal contrast, they were completely unaffected by eye
255 closure, despite the profound suppression of visual input from the eyelid.

256 Interestingly, while eye closure did not appear to have a major effect on the earliest
257 stages of visual processing (LGN and V1), we observed a qualitatively distinct pattern
258 within extrastriate cortices V2 and V3. When the eyes were closed, there was a drastic
259 attenuation of stimulus evoked responses, regardless of temporal contrast [Main effects
260 of eye closure: V2: $F(1,31) = 9.66$, $P = 0.0043$; V3: $F(1,31) = 10.42$, $P = 0.003$; Main effect
261 of temporal contrast V2: $F(1,31) = 5.54$, $P = 0.025$; V3: $F(1,31) = 0.01$, $P = 0.971$].
262 Pairwise comparisons revealed a significant decrease in BOLD response to high temporal
263 contrast stimuli with eye closure in V2 ($t(14) = -3.09$; $P = 0.004$) and V3 ($t(14) = -2.89$; $P =$
264 0.005). Overall, these results indicate that visual processing appears to be qualitatively
265 different with eyes closed compared to when eyes are open. The BOLD response in LGN
266 and V1 was modulated by temporal contrast but was unaffected by eye closure, whereas
267 eye closure strongly reduced responses in extrastriate cortices V2 and V3.



268 **Figure 2. Eye closure has minimal effect on visual responses in LGN and V1, while suppressing**
 269 **responses in V2 and V3.** (A) Event-triggered average for luminance task across ROI and eye
 270 condition. Across LGN, V1, and V2, during eyes open runs high temporal contrast stimuli elicits a
 271 greater BOLD response than with low temporal contrast stimuli. Though there is no effect of temporal
 272 contrast in V3, BOLD response increases regardless of the stimulus temporal contrast. During eye
 273 closure, BOLD responses in LGN and V1 during the high temporal contrast stimuli elicits a similar
 274 BOLD response as during eyes open runs. With eye closure, V2 and V3 have strongly attenuated
 275 BOLD regardless of temporal contrast. Red plots indicate high temporal contrast trials and blue
 276 indicates the low temporal contrast trials. The grey bar indicates 16 second period of stimulus
 277 presentation. Error shading is 1 SEM. N=8 subjects. (B) Average BOLD activation during stimulus
 278 presentation across conditions. Pairwise comparisons show a significant decrease in V2 and V3 BOLD
 279 magnitude with eye closure for high temporal contrast stimuli. In LGN, BOLD magnitude with high
 280 temporal contrast stimuli with eyes open was marginally greater than low contrast ($t(14)=2.45$; $P =$
 281 0.0139) at a Bonferroni corrected p-value cutoff of 0.0125. In V1 with eyes closed, BOLD magnitude
 282 during high temporal contrast stimuli was marginally greater than during low temporal contrast stimuli
 283 ($t(14)=1.82$; $P = 0.044$). In V2, BOLD magnitude with high temporal contrast stimuli with eyes
 284 open was greater than low contrast ($t(14)=2.65$; $P = 0.009$) and high temporal contrast stimuli with eyes
 285 closed was suppressed compared to eyes open. In V3, BOLD magnitude during high temporal contrast
 286 stimuli with eyes closed was also suppressed compared to eyes open. Y-axis is BOLD signal averaged
 287 across 4-16s post-stimulus onset. Error bars are 1 SEM. All p-values from pairwise comparison only
 288 survive multiple comparison correction at a p-value less than 0.0125, using Bonferroni correction
 289 ($0.05/n$ where $n=4$ per ROI). * $P < 0.0125$
 290

291 Along with the heterogeneity in patterns observed across striate and extrastriate
292 regions, it is possible that there exists heterogeneity *within* each region. It has been
293 reported that there is an eccentricity bias of the BOLD response in V1 and V2, when
294 participants viewed center-surround stimuli with no local contrast (Cornelissen et al.,
295 2006). To test for an eccentricity bias and if eye closure impacts this bias, we separated
296 voxels in V1-V3 by their eccentricity preference, based on pRF estimates (LGN was
297 excluded from this analysis due to being underpowered for pRF analyses). We defined
298 foveally-preferring voxels as those preferring between $0.01^\circ - 1.5^\circ$ from fixation,
299 parafoveal-preferring voxels were those between $1.5^\circ - 4.0^\circ$, and peripheral-preferring
300 voxels were between $4.0^\circ - 17.0^\circ$. As low temporal contrast trials elicited no significant
301 activation across visuocortical regions, we did not test for an effect of eccentricity during
302 low temporal contrast trials. We found that the effect of eccentricity was not significant in
303 V1 [$F(2,47) = 1.23, P = 0.303$] (Figure 3), nor in V2 [$F(2,47) = 0.90, P = 0.413$] nor V3
304 [$F(2,47) = 0.84, P = 0.440$]. No ROIs had any significant interaction between eye closure
305 and eccentricity [V1: $F(2,47) = 1.23, P = 0.303$; V2: $F(2,47) = 0.47, P = 0.631$; V3: $F(2,47)$
306 $= 0.48, P = 0.620$]. This suggests that across striate and extrastriate cortices there is no
307 eccentricity bias in BOLD responses nor any difference with eye closure. Thus, the impact
308 of high temporal contrast stimuli and eye closure on BOLD appear uniform within each
309 visuocortical area.



310 **Figure 3. The effects of eye closure do not depend on eccentricity tuning.** (A) Event-triggered
 311 average for BOLD response to luminance task across cortical ROI and eye condition separated by
 312 voxels tuned to different portions of the visual field. With eyes open and eyes closed, the BOLD
 313 responses to high contrast stimuli are uniform across eccentricities for all cortical ROIs. Foveal voxels
 314 were tuned to between 0.01 dva – 1.5 dva. Parafoveal voxels were tuned to between 1.5 dva – 4.0
 315 dva. Peripheral voxels were tuned to between 4.0 dva – 17 dva. (B) Average BOLD activation during
 316 stimulus presentation across conditions (top = eyes closed; bottom = eyes open), separated by
 317 eccentricity preference. There are no significant pairwise comparisons when comparing eccentricity
 318 responses within each ROI. Y-axis is BOLD signal averaged across 4-16s post-stimulus onset. Error
 319 bars and error shading is 1 SEM.

320

321 Discussion

322 With subjective experience it is clear that we can still perceive visual stimuli with closed
 323 eyes, but how distinct stages of the visual system supported this filtered visual experience
 324 was unknown. In this study, we found that eye closure produces a qualitatively distinct
 325 pattern of modulatory responses within the early visual system: closing one's eyes

326 selectively attenuated luminance processing in extrastriate cortex, but not in LGN nor
327 striate cortex.

328 In line with previous literature showing that early visual responses can still occur
329 when the eyes are closed (Marx et al., 2003; Sharon & Nir, 2018), we demonstrated that
330 with closed eyes, luminance-dependent responses remain present in the LGN and V1.
331 However, we found substantial heterogeneity in activation across regions when eyes
332 were closed. One hypothesis as to why we observed strongly attenuated BOLD with
333 closed eyes in extrastriate cortex, but not the LGN nor striate cortex, is that top-down
334 modulation of visuocortical responses is often stronger in extrastriate compared to striate
335 cortex (Haenny & Schiller, 1988; Moran & Desimone, 1985; Shulman et al., 1997). It has
336 been demonstrated that higher-order sensory regions, such as the frontal eye field (FEF),
337 may account for the selective top-down modulation of extrastriate cortical responses
338 (Veniero et al., 2021). Resting-state fMRI studies that examined altered functional
339 connectivity between eyes open and closed states found increased activation of the FEF
340 during eyes closed relative to eyes open scans (Weng et al., 2020), lending further
341 support to top-down modulation of extrastriate cortex during eyes closed states.
342 Interestingly, one study which microstimulated the FEF of monkeys and measured
343 visuocortical responses with fMRI found that FEF stimulation modulated extrastriate
344 areas only in the presence of a visual stimulus, indicating that top-down modulation of the
345 extrastriate cortices is dependent on bottom-up influence (Ekstrom et al., 2008). Since
346 our paradigm includes a visual stimulus, it is possible that eye closure in the presence of
347 visual stimuli attenuates extrastriate cortical responses through both top-down and
348 bottom-up mechanisms. The eyelid abolishes almost all structure and form-like
349 information, which is necessary to elicit responses in extrastriate cortices that prefer
350 higher-level feature selectivity, such as spatial contrast, shapes, and contours. However,
351 eyelid closure still passes through luminance information, which is known to activate
352 striate cortex (Vinke & Ling, 2020). This preservation of luminance information, but
353 attenuation of higher-level information, may explain the preservation of early visual
354 pathway activation with weakened extrastriate activation.

355 Visuocortical responses have been shown to depend on luminance modulation,
356 with responses increasing monotonically with luminance (Vinke & Ling, 2020). In addition

357 to luminance modulation, luminance response functions are strongly contrast dependent,
358 with lower spatial contrast drastically decreasing visuocortical responses to luminance
359 (Vinke & Ling, 2020). Since the eyelid filters out much visual information, it is likely that
360 spatial contrast no longer impacts visual responses and that luminance information
361 dominates what might pass through the eyelid. Additionally, the lower luminance retinal
362 input with eye closure cannot fully explain our results since LGN and V1 showed no
363 significant change in BOLD activation between open and closed eye conditions. Since
364 the eyelid is characterized as a red-pass filter (Ando & Kripke, 1996), it is possible that
365 early visual pathways preferentially process this red visual content that extrastriate cortex
366 is blind to; however, to our knowledge no evidence of this exists. Although further work
367 will be needed to better unpack luminance responses in the early visual system, our
368 results suggest that luminance-based responses within early visual areas may not always
369 necessitate the existence of spatial contrast in order to reveal themselves, as previously
370 suggested.

371 One interpretation of our results is that that modulation of visual processing during
372 eye closure may be dependent on brain state, not just the physical barrier of the eyelid.
373 Eye closure likely induces a change in overall brain state that alters both the processing
374 of visual information and large-scale functional network processing. Eye closure
375 decreases activity in attentional systems in the occipital and parietal lobes and increases
376 functional coupling between sensory thalamus and somatosensory regions (Marx et al.,
377 2003; Wei et al., 2018; Weng et al., 2020). These differences in spontaneous brain activity
378 across sensory and attentional systems point to altered brain states with eye closure.
379 Exteroceptive and interoceptive mental state hypotheses have been formulated where an
380 exteroceptive mental state is characterized by increased attention and sensory
381 processing of the external environment with eyes open (Marx et al., 2003). On the other
382 hand, an interoceptive mental state is characterized by internally-directed cognition and
383 reduced sensory processing with eyes closed. Many brain states require prolonged
384 periods of eye closure, such as sleep and meditation, that involve reduced sensory
385 awareness of external stimuli and enhanced internally-directed attention. Thus, eye
386 closure may modulate visual processing through attentional or brain-state-dependent
387 mechanisms.

388 **Author contributions:**

389 Conceptualization, N.G.C, M.K., L.D.L., and S.L.; Methodology, N.G.C., M.K., L.D.L., and
390 S.L.; Investigation, N.G.C and M.K.; Writing – Original Draft, N.G.C, M.K., L.D.L., and
391 S.L.; Writing – Review & Editing, N.G.C, M.K., L.D.L., and S.L.; Funding Acquisition,
392 L.D.L. and S.L.; Supervision, L.D.L. and S.L.

393

394

395 Further information and requests for resources should be directed to and will be fulfilled
396 by the lead contact, Sam Ling (samling@bu.edu).

397 **References**

- 398 Andersson, J. L. R., Skare, S., & Ashburner, J. (2003). How to correct susceptibility
399 distortions in spin-echo echo-planar images: Application to diffusion tensor imaging.
400 *NeuroImage*, 20(2), 870–888. [https://doi.org/10.1016/S1053-8119\(03\)00336-7](https://doi.org/10.1016/S1053-8119(03)00336-7)
- 401 Ando, K., & Kripke, D. F. (1996). *Light Attenuation by the Human Eyelid*.
- 402 Bierman, A., Figueiro, M. G., & Rea, M. S. (2011). Measuring and predicting eyelid
403 spectral transmittance. *Journal of Biomedical Optics*, 16(6), 067011.
404 <https://doi.org/10.1117/1.3593151>
- 405 Blume, C., Garbazza, C., & Spitschan, M. (2019). Effects of light on human circadian
406 rhythms, sleep and mood. In *Somnologie* (Vol. 23, Issue 3, pp. 147–156). Dr. Dietrich
407 Steinkopff Verlag GmbH and Co. KG. <https://doi.org/10.1007/s11818-019-00215-x>
- 408 Brainard, D. H. (1997). The Psychophysics Toolbox. *Spatial Vision*, 10(4), 433–436.
409 <https://doi.org/10.1163/156856897X00357>
- 410 Cornelissen, F. W., Wade, A. R., Vladusich, T., Dougherty, R. F., & Wandell, B. A. (2006).
411 No functional magnetic resonance imaging evidence for brightness and color filling-
412 in in early human visual cortex. *Journal of Neuroscience*, 26, 3634-3641.
413 <https://doi.org/10.1523/JNEUROSCI.4382-05.2006>
- 414 Dumoulin, S. O. & Wandell, B. A. (2008). Population receptive field estimates in human
415 visual cortex. *NeuroImage*, 39, 647-660.
416 <https://doi.org/10.1016/j.neuroimage.2007.09.034>
- 417 Ekstrom, L. B., Roelfsema, P. R., Arsenault, J. T., Bonmassar, G., & Vanduffel, W. (2008).
418 Bottom-up dependent gating of frontal signals in early visual cortex. *Science*, 321,
419 414-417. doi: 10.1126/science.1153276
- 420 Fischl, B. (2012). FreeSurfer. *Neuroimage* 62:774–781.
- 421 Fujita, N., Tanaka, H., Takanashi, M., Hirabuki, N., Abe, K., Yoshimura, H., & Nakamura,
422 H. (2001). Lateral geniculate nucleus: Anatomic and functional identification by use
423 of MR imaging. *American Journal of Neuroradiology*, 22, 1719-1726. PMID:
424 PMC7974446
- 425 Greve, D. N., & Fischl, B. (2009) Accurate and robust brain image alignment using
426 boundary-based registration. *Neuroimage*, 48, 63–72.

- 427 Haenny, P. E., & Schiller, P. H. (1988). State dependent activity in monkey visual cortex.
428 *Experimental Brain Research*, 69(2), 225–244. <https://doi.org/10.1007/BF00247569>
- 429 Kay, K. N., Winawer, J., Mezer, A., & Wandell, B. A. (2013). Compressive spatial
430 summation in human visual cortex. *J Neurophysiol*, 110, 481–494.
431 <https://doi.org/10.1152/jn.00105.2013>.-Neurons
- 432 Ling, S., Pratte, M. S., & Tong, F. (2015). Attention alters orientation processing in the
433 human lateral geniculate nucleus. *Nature Neuroscience*, 18(4), 496–498.
434 <https://doi.org/10.1038/nn.3967>
- 435 Marx, E., Deutschländer, A., Stephan, T., Dieterich, M., Wiesmann, M., & Brandt, T.
436 (2003). Eyes open and eyes closed as rest conditions: Impact on brain activation
437 patterns. *NeuroImage*, 21(4), 1818–1824.
438 <https://doi.org/10.1016/j.neuroimage.2003.12.026>
- 439 Moran, J., & Desimone, R. (1985). Selective Attention Gates Visual Processing in the
440 Extrastriate Cortex. *Science*, 229(4715), 782–784.
441 <https://doi.org/10.1126/science.4023713>
- 442 Ohayon, M. M., & Myles, C. (2016). Artificial outdoor nighttime lights associate with
443 altered sleep behavior in the American general population. *Sleep*, 39(6), 1311–1320.
444 <https://doi.org/10.5665/sleep.5860>
- 445 Sharon, O. & Nir, Y. (2018). Attenuated fast steady-state visual evoked potentials during
446 human sleep. *Cerebral Cortex*, 28, 1297–1311. doi:10.1093/cercor.bhx043
- 447 Shulman, G., Corbetta, M., Buckner, R. L., Raichle, M. E., Fiez, J. A., Miezin, F. M., &
448 Petersen, S. E. (1997). Top-down modulation of early sensory cortex. *Cerebral*
449 *Cortex*, 7(3), 193–206. <https://doi.org/10.1093/cercor/7.3.193>
- 450 Veniero, D., Gross, J., Morand, S., Duecker, F., Sack, A. T., & Thut, G. (2021). Top-down
451 control of visual cortex by the frontal eye fields through oscillatory realignment.
452 *Nature Communications*, 12(1). <https://doi.org/10.1038/s41467-021-21979-7>
- 453 Vinke, L. N., & Ling, S. (2020). Luminance potentiates human visuocortical responses.
454 2020. *First Published De-Cember*, 123, 473–483.
455 <https://doi.org/10.1152/jn.00589.2019>.-Our
- 456 Wei, J., Chen, T., Li, C., Liu, G., Qiu, J., & Wei, D. (2018). Eyes-open and eyes-closed
457 resting states with opposite brain activity in sensorimotor and occipital regions:

458 Multidimensional evidences from machine learning perspective. *Frontiers in Human*
459 *Neuroscience*, 12. <https://doi.org/10.3389/fnhum.2018.00422>
460 Weng, Y., Liu, X., Hu, H., Huang, H., Zheng, S., Chen, Q., Song, J., Cao, B., Wang, J.,
461 Wang, S., & Huang, R. (2020). Open eyes and closed eyes elicit different temporal
462 properties of brain functional networks. *NeuroImage*, 222.
463 <https://doi.org/10.1016/j.neuroimage.2020.117230>
464 Yeo, B. T., Krienen, F. M., Sepulcre, J., Sabuncu, M. R., Lashkari D., Hollinshead, M.,
465 Roffman, J. L., Smoller, J. W., Zöllei, L., Polimeni, J. R., Fischl, B., Liu, H., & Buckner,
466 R. L. (2011) The organization of the human cerebral cortex estimated by intrinsic
467 functional connectivity. *J Neurophysiol*, 106, 1125–1165.